Research article

Traffic conflict assessment for non-lane-based movements of motorcycles under congested conditions

Long Xuan Nguyen [a,*], Shinya Hanaoka [b,1], Tomoya Kawasaki [c,2]

[a] Department of Civil and Environmental Engineering, Tokyo Institute of Technology, 2-12-1, O-okayama, Meguro-ku, Tokyo 152-8550, Japan
[b] Department of International Development Engineering, Tokyo Institute of Technology, 2-12-1, O-okayama, Meguro-ku, Tokyo 152-8550, Japan
[c] Department of Transportation Systems Engineering, Nihon University, 744-7-24-1, Narashino-dai, Funabashi, Chiba, 274-8501, Japan

ARTICLE INFO

ABSTRACT

Traffic conflict under congested conditions is one of the main safety issues of motorcycle traffic in developing countries. Unlike cars, motorcycles often display non-lane-based movements such as swerving or oblique following of a lead vehicle when traffic becomes congested. Very few studies have quantitatively evaluated the effects of such non-lane-based movements on traffic conflict. Therefore, in this study we aim to develop an integrated model to assess the traffic conflict of motorcycles under congested conditions. The proposed model includes a concept of safety space to describe the non-lane-based movements unique to motorcycles, new features developed for traffic conflict assessment such as parameters of acceleration and deceleration, and the conditions for choosing a lead vehicle. Calibration data were extracted from video clips taken at two road segments in Ho Chi Minh City. A simulation based on the model was developed to verify the dynamic non-lane-based movements of motorcycles. Subsequently, the assessment of traffic conflict was validated by calculating the probability of sudden braking at each time interval according to the change in the density of motorcycle flow. Our findings underscore the fact that higher flow density may lead to conflicts associated with a greater probability of sudden breaking. Three types of motorcycle traffic conflicts were confirmed, and the proportions of each type were calculated and discussed.

1. Introduction

Motorcycles are the main mode of transportation in several developing Asian countries. The basic difference in the movement of a car and that of a motorcycle relates to lane-based and non-lane-based movements, respectively. A car runs in and seldom changes lanes. However, a motorcycle frequently changes direction, especially under congested conditions. When a road lacks a motorcycle lane, a motorcycle need not follow lane discipline. For example, a motorcycle may travel alongside other vehicles in the same lane [1] or obliquely follow a lead vehicle [2]. Such non-lane-based movements of motorcycles are unique and influence the likelihood of traffic accidents. Hence, in this study, we focus on the effects of such non-lane-based movements on traffic conflict under congested situations.

Many researchers have attempted to represent non-lane-based movements by separating them into longitudinal and lateral movements. Because longitudinal movement resembles car following, the traditional car-following model has been used to describe this movement. However, when modeling lateral movement, many different models have been developed on the basis of different assumptions regarding the relationship between longitudinal and lateral movements. Cho and Wu [3] assumed that the lateral position of a motorcycle was determined by the average lateral position of the surrounding vehicles weighted by their longitudinal positions. Minh et al. [4,5] supposed that a motorcycle runs on a "dynamic lane" to follow a lead motorcycle on the same dynamic lane or change lanes to overtake its leader. The width of the dynamic lane was calculated using the linear relationship between the distance separating two vehicles running side-by-side and the average speed. Lan and Chang [6] developed a cellular automation model to simulate two-dimensional motorcycle movements. They set the size of a cell unit to 1.25 m × 1.25 m to represent a motorcycle as 2 × 1 cell units. A motorcycle can then move from one cell to another based on simple moving rules developed for motorcycles, such as car-following, lane-changing, or overtaking. Moreover, most models do not consider safety factors such as reaction time, safety distance,

* Corresponding author. Tel./fax: +81 35 734 2575.
  E-mail addresses: nguyen@tp.ide.titech.ac.jp (L.X. Nguyen), hanaoka@ide.titech.ac.jp (S. Hanaoka), kawasaki.tomoya@nihon-u.ac.jp (T. Kawasaki).
  [1] Tel./fax: +81 35 734 3468.
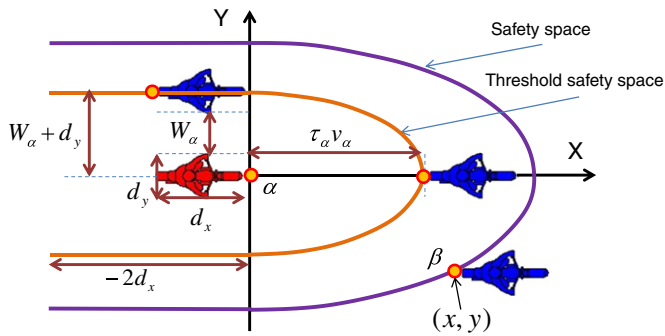 [2] Tel./fax: +81 47 469 5219.

Fig. 1. Safety space and the threshold safety space.

or speed difference related to the description of collision avoidance behavior. Nguyen et al. [14] proposed the concept of a safety space in which longitudinal and lateral movements can be integrated. This model has the potential to evaluate the safety issues of non-lane based motorcycle movements.

The safety level of a vehicle is denoted by the number or rate of accidents involved with the vehicle. There are two popular approaches for estimating the safety level of a vehicle: (1) development of safety performance functions that relate the number or rate of accidents to the explanatory variables by using regression analysis, and (2) development of simulation models to calculate the safety level through measures for traffic safety assessment. In the former, correlations among variables are found by analyzing the dispersion and approximated by deriving regression formulas. Neuman and Glennon [7] found correlations among the road environment of road design, infrastructure, and accident causes. Warshawsky-Livne and Shinar [8] found relationships between the reaction time to a brake light and the driver's gender, age, level of expectancy for the brake light, as well as the number of times that a task was performed. However, this approach requires consensus data on traffic accidents, which are very difficult to collect in most developing Asian countries. In reality, the probability of a traffic

accident is very low and varies across the time of day, day of week, location, and events. The latter approach has the potential to address the aforementioned lack of observation data. Simulation models were developed on the basis of behavioral modeling of the vehicles. Although these models cannot estimate the number of accidents, they can be used to assess the safety level or higher-than-average accident rates [9]. Simulation models can efficiently produce a larger amount of analysis data than observation data, with time savings. Moreover, these models cover many scenarios such as nighttime, weekends, and special locations, for which observers face difficulties in collecting data.

Conventional studies have focused on developing techniques for measuring traffic conflict [10–12] to evaluate the safety level of a vehicle. A traffic conflict is defined as an event that involves two or more road users, in which the action of one user causes another to make an evasive maneuver to avoid a collision [13]. The primary measures to determine a conflict by using microscopic simulation were summarized by Gettman and Head [9] as time-to-collision (TTC), post-encroachment time (PET), maximum of the speeds of two vehicles involved in the conflict event (MaxS), maximum relative speeds of two vehicles involved in the conflict event (DeltaS), and deceleration rate (DR). These values are available from the output of the simulation model at every time step. For this reason, here, we use DR as an efficient measure to assess the traffic conflict of motorcycles at a road segment.

In this study, we aim to develop a model to assess the traffic conflict of motorcycles. The proposed model consists of a concept of safety space to describe non-lane-based movements, which are unique to motorcycles in congested situations. New features are also developed for traffic conflict assessment, such as parameters of acceleration and deceleration as well as the following conditions for choosing a lead vehicle: (1) the following angle, and (2) the following route width. Calibration for parameter estimation is explained using the trajectory data of moving motorcycles observed from video images at two different road segments in Ho Chi Minh City. For model verification, a simulator is developed to verify the dynamic non-lane-based movements of motorcycles: swerving and oblique following. An assessment of traffic conflict caused by these movements is validated by calculating the DR at each time interval according to the change in density of the motorcycle flow.

2. Model development

2.1. Concept of safety space for depicting non-lane-based movements of motorcycles

The concept of safety space developed by Nguyen et al. [14] is used to describe the behaviors of increasing or decreasing speed for non-lane-based motorcycle movements. It consists of the following three assumptions:

Assumption 1. Safety space is the space that surrounds a single motorcycle running along a road. The boundary of the space, which is determined by the influence of other vehicles on the driving behaviors of the subject vehicle, is assumed to be the equipotential line; that is, all vehicles on the same line represent the same level of safety. In this study, the safety space for a subject motorcycle is assumed to be determined by the combination of a half-ellipsoidal boundary and two parallel lines, as illustrated in Fig. 1. The ellipsoidal boundary shows the space when a preceding motorcycle runs in front of the subject. Two parallel lines constitute the clearances on both sides of the subject when two vehicles run side-by-side.

The "threshold" safety space is introduced to define the minimal safety level that a motorcyclist considers acceptable for driving and avoiding a possible accident. As shown in Fig. 1, the threshold safety space of a subject vehicle α is assumed to have an ellipsoidal shape, with the vehicle placed at the center and the direction of its velocity v_α determining the direction of the major axis. The length of the semi-major axis, which is the safety distance on the x-axis measured from the front of one motorist to the rear of another, is expressed as $\tau_\alpha v_\alpha$, where τ_α is the relaxation time for α. *The relaxation time is defined as the time required to complete the following series of actions to avoid a collision: perceive a lead vehicle braking suddenly, swerve left or right, and brake to reduce speed.* The length of the semi-minor axis is the safety distance on the y-axis, given by $W_\alpha + d_y$, where W_α is the lateral distance on the y-axis between the subject motorcycle and another vehicle. The physical size of a motorcycle on each axis is denoted by d_x, d_y.

Assumption 2. When another vehicle moves closer to or farther away from a subject vehicle, the safety space becomes smaller or larger, respectively; as a result, the safety level decreases or increases. A motorcyclist is simply assumed to accelerate or decelerate in response to changes in the safety level with a view to achieving a higher safety level.

Suppose that a subject motorcycle α travels at speed v_α at time t. If an influential motorcycle β increases or decreases its speed to v_β at time t, then α will adjust its acceleration a_α, with a time lag T, to be equal to the rate of change in safety level V_β for the current position of β in the direction of the

relative speed vector $\vec{v}_{\alpha\beta} = \vec{v}_\beta - \vec{v}_\alpha$. If V_β is assumed to be an exponential function of the safety space with a half-ellipsoidal boundary connected to two parallel lines, the lengths of which are equal to twice the length of the subject vehicle, then acceleration a_α is formulated as follows:

$$a_\alpha(t+T) = -\nabla_{\vec{v}_{\alpha\beta}} V_\beta = \begin{cases} -\nabla_{\vec{v}_{\alpha\beta}}\left(A\exp\left(-\left(\dfrac{x^2}{(\tau_\alpha v_\alpha)^2} + \dfrac{y^2}{\left(W_\alpha + d_y\right)^2}\right)\right)/B\right) & \text{if } x \geq 0 \\[3mm] -\nabla_{\vec{v}_{\alpha\beta}}\left(A\exp\left(-\left(\dfrac{y^2}{\left(W_\alpha + d_y\right)^2}\right)/B\right)\right) & \text{if } -2d_x \leq x \leq 0 \end{cases}$$

(1)

where $\nabla_{\vec{v}_{\alpha\beta}}$ indicates the directional derivative of safety level V_β in the direction of relative speed vector $\vec{v}_{\alpha\beta}$. A and B are parameters that represent the magnitude of the safety level, respectively. x and y are the distances between vehicles α and β measured on the x-axis and y-axis, respectively. The direction of the acceleration vector, $\vec{a}_\alpha$ (i.e., the direction of motion), is assumed to be the direction of the gradient of safety level. This assumption is expressed as follows:

$$\frac{\vec{a}_\alpha}{a_\alpha} = \begin{cases} \dfrac{\nabla V_\beta}{\|\nabla V_\beta\|} & \text{if } a_\alpha \leq 0 \\[3mm] \dfrac{-\nabla V_\beta}{\|\nabla V_\beta\|} & \text{if } a_\alpha > 0 \end{cases}$$

(2)

where ∇V_β and ∇V_β denote the gradient vector of V_β and its magnitude, respectively. Eq. (2) shows a simple assumption. When β moves closer, α will decelerate ($a_\alpha \leq 0$) and move farther away from β in the gradient direction to avoid a collision. When β moves farther away, α will accelerate ($a_\alpha > 0$) to follow β in the reverse gradient direction.

Assumption 3. Under heavy traffic conditions, a motorcycle responds to the most influential motorcycle at a certain time. We can assume that a motorcycle is chosen to be the most influential if a subject vehicle responds to it with the maximum acceleration. This assumption is reasonable because a subject motorcycle may be unable to respond to many influential motorcycles simultaneously, especially under congested conditions. It focuses on reducing speed to avoid a collision with the most influential while paying less attention to others. It also increases its speed to follow the most influential motorcycle and achieve the highest acceleration.

The proposed model mentioned in this section is based on Nguyen et al. [14]. In the next section, we will introduce two new points to increase the accuracy of results estimated by the proposed model: (1) distinguish parameters for acceleration and deceleration, and (2) modify the conditions for selecting the most influential motorcycle by the angle and route width.

2.2. Parameters for acceleration and deceleration

According to previous proposals by Ahmed [15] and Toledo et al. [16], when a motorcyclist responds to changes in the speed of a leader, two different natural motivations may arise to accelerate or decelerate. Whereas acceleration is likely to obtain the desired speed, applying the brakes is likely to avoid collisions. Hence, two different parameter sets were introduced to represent the difference in numerical values between acceleration and deceleration. Eq. (1) is rewritten after taking the derivative, as follows:

$$a_\alpha = \begin{cases} A\exp\left(-\left(\dfrac{x^2}{(\tau_\alpha v_\alpha)^2} + \dfrac{y^2}{\left(W_\alpha + d_y\right)^2}\right)\right)/B \left(v_{\alpha\beta}\right)^{-1}\left(\dfrac{xv_x}{(\tau_\alpha v_\alpha)^2} + \dfrac{yv_y}{\left(W_\alpha + d_y\right)^2}\right) & \text{if } x \geq 0 \\[3mm] A\exp\left(-\left(\dfrac{y^2}{\left(W_\alpha + d_y\right)^2}\right)\right)/B \left(v_{\alpha\beta}\right)^{-1}\left(\dfrac{yv_y}{\left(W_\alpha + d_y\right)^2}\right) & \text{if } -2d_x \leq x < 0 \end{cases}$$

(3)

where v_x and v_y are the relative speeds between a subject motorcycle and an influential motorcycle in the x- and y-axis directions, respectively. The difference in numerical values between acceleration and deceleration is represented by replacing the original parameter set (A, B) in Eq. (3) with two new parameter sets (A_{acc}, B_{acc}) and (A_{dec}, B_{dec}). When the acceleration is positive, i.e.,

$$\frac{xv_x}{(\tau_\alpha v_\alpha)^2} + \frac{yv_y}{\left(W_\alpha + d_y\right)^2} \geq 0,$$

then

$$a_\alpha = \begin{cases} A_{acc}\exp\left(-\left(\dfrac{x^2}{(\tau_\alpha v_\alpha)^2} + \dfrac{y^2}{\left(W_\alpha + d_y\right)^2}\right)\right)/B_{acc} \left(v_{\alpha\beta}\right)^{-1}\left(\dfrac{xv_x}{(\tau_\alpha v_\alpha)^2} + \dfrac{yv_y}{\left(W_\alpha + d_y\right)^2}\right) & \text{if } x \geq 0 \\[3mm] A_{acc}\exp\left(-\left(\dfrac{y^2}{\left(W_\alpha + d_y\right)^2}\right)\right)/B_{acc} \left(v_{\alpha\beta}\right)^{-1}\left(\dfrac{yv_y}{\left(W_\alpha + d_y\right)^2}\right) & \text{if } -2d_x \leq x < 0 \end{cases}$$

(4a)

When the acceleration is negative, i.e.,

$$\frac{xv_x}{(\tau_\alpha v_\alpha)^2} + \frac{yv_y}{\left(W_\alpha + d_y\right)^2} < 0,$$

then

$$a_\alpha = \begin{cases} A_{dec} \exp\left(-\left(\dfrac{x^2}{(\tau_\alpha v_\alpha)^2} + \dfrac{y^2}{\left(W_\alpha + d_y\right)^2}\right)/B_{dec}\right)(v_{\alpha\beta})^{-1}\left(\dfrac{xv_x}{(\tau_\alpha v_\alpha)^2} + \dfrac{yv_y}{\left(W_\alpha + d_y\right)^2}\right) & \text{if } x \geq 0 \\ A_{dec} \exp\left(-\left(\dfrac{y^2}{\left(W_\alpha + d_y\right)^2}\right)/B_{dec}\right)(v_{\alpha\beta})^{-1}\left(\dfrac{yv_y}{\left(W_\alpha + d_y\right)^2}\right) & \text{if } -2d_x \leq x < 0 \end{cases}. \tag{4b}$$

Eq. (4a) shows that a subject vehicle will accelerate when an influential vehicle in front of it moves out of the safety space. The deceleration denoted by Eq. (4b) will increase when an influential motorcycle moves into the safety space, and then gradually decreases to zero when the distance between the two motorcycles is zero. This assumption is reasonable because a subject vehicle brakes to avoid an accident when approaching a lead motorcycle, and then it swerves left or right and releases the brake when running beside the lead.

2.3. Conditions for selecting the most influential vehicle to accelerate

As mentioned in Assumption 3, we modified the conditions for selecting the most influential motorcycle in consideration of two physical conditions: the following angle, and the width of route to follow a leader. These conditions are described below.

2.3.1. Following angle φ_0

A motorcyclist feels safe and comfortable to increase speed when following a leader ahead at an angle φ_α, which is smaller than the following angle φ_0 (see Fig. 2). The angle φ_α is related to the angle of swerving and should have an upper limit. The angle φ_0 refers to the maximum swerving angle when a vehicle turns left or right to follow its leader. Neglecting this condition may result in a situation in which a motorcycle accelerates to follow its leader running beside only by increasing speed in the horizontal direction of movement. In practice, motorcycles prefer to follow the leader in a nearly straight route.

2.3.2. Following route width RW_0

A motorcycle speeds up and follows a vehicle ahead if there are no other vehicles on the following route. Considering motorcycle number 4 in Fig. 3, the subject vehicle could not follow it because vehicle number 2 and motorcycle number 3 are inside the following route. The width RW_0 of the following route is introduced to determine whether there are obstacles on the following route. The conditions are examined after every simulation time step of 0.5 s by using trajectory data obtained from video images when calibrating the parameters. According to Assumption 3, a subject motorcycle prefers to follow the leader, i.e., the most influential motorcycle, which is sometimes the furthest vehicle away. However, it cannot do so when there are many other motorcycles between it and the leader.

3. Model calibration

To calibrate the proposed model, data on vehicle trajectories over time are necessary. Therefore, time-series trajectory data for each vehicle were recorded using a video camera. Because the study only covers situations of congested motorcycle traffic, observations of uncongested situations and those in which cars and bicycles were present were excluded from the video clips.

3.1. Data collection

Ho Chi Minh City, which has a high number of motorcycles, is a good location to conduct the survey. Two road segments on Phan Dang Luu Street and Cong Hoa Street were 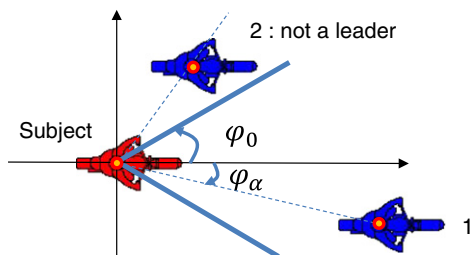selected for data collection. The first road segment is near an intersection and is 8.4 m wide. This segment has only one lane in the observed direction and motorcycles run at an average speed of 20 km/h. The second road segment has three lanes in each direction, each lane being 3.65 m wide. The segment is about 100 m from the nearest intersection. Motorcycles run at an average speed of 30 km/h and are allowed to use any lane that is available.

Time-series trajectory data for each vehicle were recorded using a video camera. The video recorder was set up on a high building near the study location. Image video files with a resolution of 1280 × 720 pixels were made to track vehicle trajectories. The resolutions of the video image related to the real sizes of two survey locations ranges from around 30 to 100 mm/pixel. Under ideal situations, the tracking data errors are assumed to be on the order of a single pixel. Therefore, the data tracking method in this study can provide data sets with high accuracy. Vehicle movements on a 40-m-long road segment in the study direction were captured on video camera at 30 frames/s. The investigation was conducted in the period of December 30–31, 2010, from 6:00 am to 8:00 am and 3:30 pm to 5:30 pm, to record motorcycle movements during peak hours. Finally, two video clips covering a total of 4 h were obtained from two road segments.

The speed estimation from video data (SEV) software developed by Minh et al. [4] is used to track the trajectory of a subject vehicle and its surrounding vehicles. A photo of the positions of a subject motorcycle and other influential motorcycles at a given time is identified as one observation. The next observation of the same subject vehicle is collected after 0.5 s. The study collected 7 to 10 observations for each subject
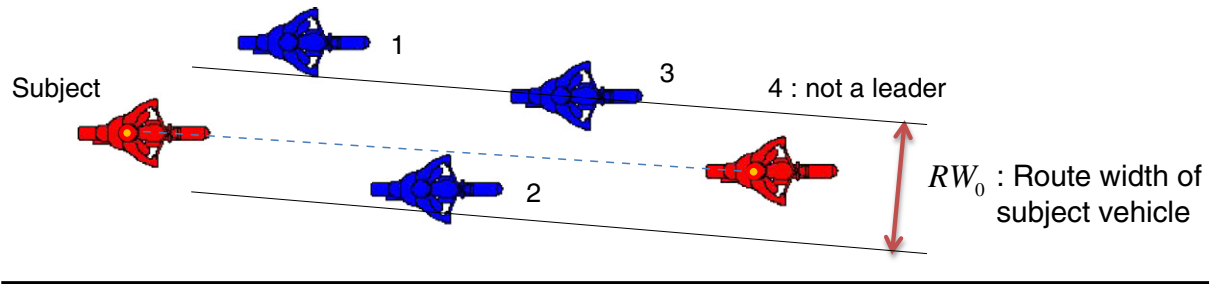
Fig. 2. Following angle of motorcycle.

Fig. 3. Following route for motorcycle to follow a leader.

vehicle. Observations during uncongested conditions and observations with bicycles, busses, and trucks were excluded from the data sample. As a result, 828 observations of 144 motorcycles on Phan Dang Luu Street and 579 observations of 152 motorcycles on Cong Hoa Street were used to estimate the parameters of the proposed model. Although more motorcycles could have been considered, a larger sample would likely have made little difference to the results given the numerous observations conducted.

3.2. Parameter calibration

The proposed model was calibrated by regression analysis. The model is formulated in Eqs. (4a) and (4b). Speed and acceleration were calculated from the trajectory data. These values and the x-y coordinates of the trajectory were considered as observed variables in the regression equation. Conditions for choosing the lead motorcycles were considered to exclude inappropriate leaders. To simplify the calculation of the nonlinear function, all drivers were assumed to have the same reaction time T and several parameters were assumed to be constant (see Table 1). The reaction time of a motorcycle is taken to be equal to the mean of the reaction time distribution, i.e., 0.5 s [4]. The lateral distance of the threshold safety space was measured from the field to be 1.8 m on average for two vehicles riding side by side. The average size of real motorcycles in the field is used for the parameter values of vehicle size. To achieve small errors of the estimation result through trial and error, the following angle is set to 30° and the following route width to 2.0 m.

SPSS software was used to derive all other parameters by solving the nonlinear regression problem (Table 2). All parameters are statistically significant at the level of 0.01, except for parameter B_{acc} on Cong Hoa Street, for which the t-value is 1.85. The signs of parameters A, B, and τ are positive because the magnitude of the safety space must have positive values. The relaxation times (τ values) observed at the two different locations were estimated to be 0.498 s and 0.496 s. Relaxation time is defined as the time required to combine steering (to change direction) and braking (to change speed) to avoid a possible collision; hence, it does not differ for different locations. The estimated relaxation time is nearly equal to the reaction time of 0.5 s. The values of parameters B_{acc} and B_{dec} are almost the same at the two locations. The difference in the values of parameters A_{acc} and A_{dec} shows that the acceleration rate

for drivers on Cong Hoa Street is greater than that of drivers on Phan Dang Luu Street. Cong Hoa Street has three lanes with vehicles traveling at an average speed of 30 km/h, which is higher than the 20 km/h on Phan Dang Luu Street. Therefore, a higher average speed implies a greater rate of acceleration.

4. Simulation results of traffic conflict assessment

4.1. Simulator

In this study, we developed a microscopic simulator based on the proposed model to assess the traffic conflict of motorcycle traffic flow at a road segment. The simulator used the open source software first introduced for simulating pedestrians by Helbing and Molnar [17] because of its flexibility and similar design features for modeling non-lane-based movements. The simulation program was written in C and run in the Linux operating system. In this section, the overall design of the simulator is presented. The components of each step of the design process are then explained.

4.1.1. Overall design

The overall design consists of the input data and a loop-over process of acceleration calculations and simulation outputs at every simulation time step (Fig. 4). The simulator can input network information data, such as the length and width of a road segment, origin–destination points, values of the safety space parameters, and free speed of motorcycles. The vehicles are then generated at the original points when a time series of traffic rate on a road segment is entered as input. The calculation process combines two different models: (1) a free acceleration model for describing the behavior of increasing speed to achieve free speed when no influential motorcycles are in front of the subject motorcycle, and (2) the proposed model for describing acceleration or deceleration when influential motorcycles appear. After calculating acceleration, the system updates the speeds and determines the next vehicle movements. The vehicles are removed from the road segment when they arrive at their destinations. The output of the program can show x, y coordinate values, speed, acceleration of all vehicles on a road over time, traffic volume, and density of the traffic flow. The simulator updates the calculation progress and output at 0.01 s interval until restraint conditions such as the maximum simulation time, maximum number of iterations, or maximum number of vehicles are reached.

Table 1
Given parameters when distinguishing acceleration and deceleration.

Parameter	Value
Reaction time T (s)	0.5
Lateral distance W (m)	1.8
Vehicle size d_x (m), d_y (m)	length = 1.9, width = 0.8
Following angle (°)	30
Following route width (m)	2.0

Table 2
Estimated parameters when distinguishing acceleration and deceleration.

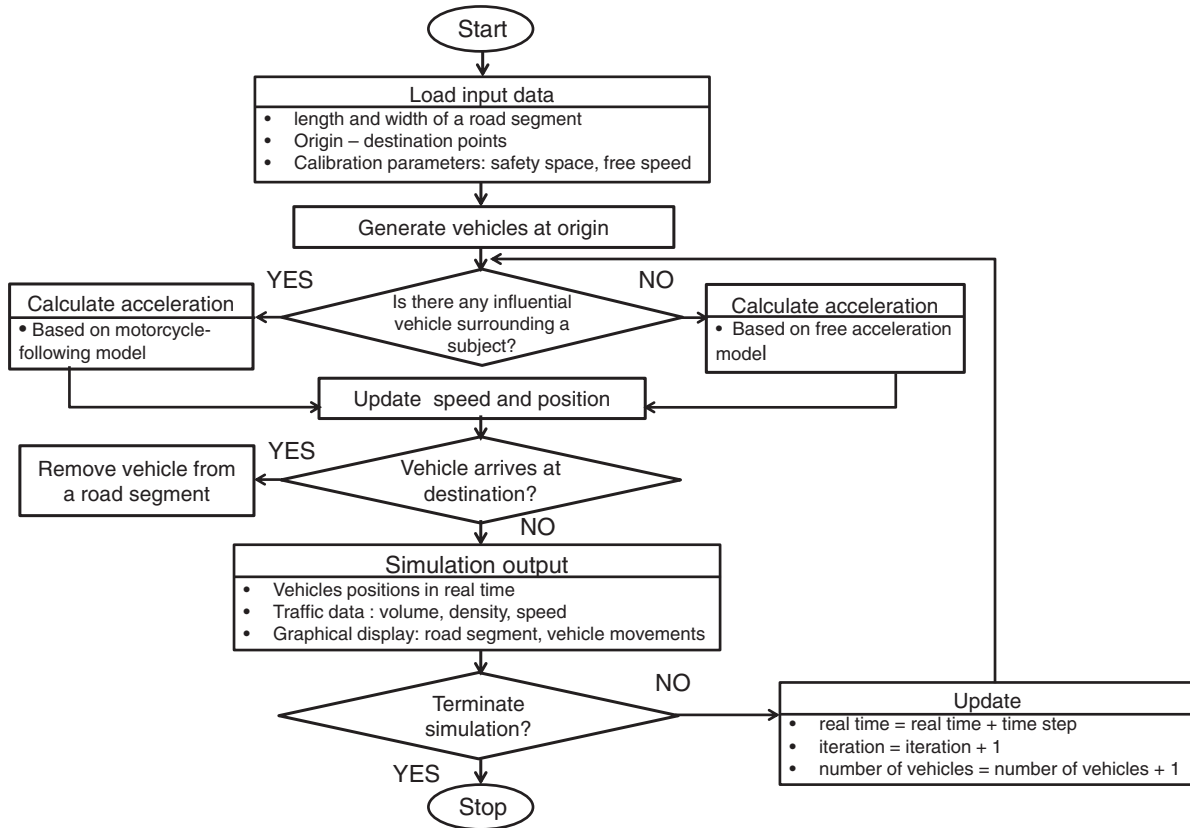| Parameter	Phan Dang Luu Street			Cong Hoa Street		
	Estimate	Std. Error	t-Value	Estimate	Std. Error	t-Value
A_{acc}	2.535	0.396	6.40	4.480	0.708	6.33
B_{acc}	5.269	1.219	4.32	5.285	2.862	1.85
A_{dec}	13.542	3.628	3.73	20.156	5.924	3.40
B_{dec}	0.132	0.031	4.27	0.151	0.034	3.85
τ (s)	0.498	0.037	13.31	0.496	0.038	12.93

Fig. 4. Flowchart of traffic simulation model.

4.1.2. Network

A straight road segment with 200 m in length and a uniform width of 5.4 m is considered. There are three pairs of origin–destination points at the two ends of the road segment. Vehicles are inserted at the origin points, run on the road segment, and are removed at the destination points. When vehicles run with free acceleration, they speed up in the direction of the road. When a vehicle approaches another, it slows down and swerves left or right. However, it cannot exit the road segment from either side because when it approaches the roadside, pushing forces in the direction perpendicular to the roadside will be activated.

4.1.3. Vehicle generation

The vehicles are generated randomly at original points. This randomness makes the initial relative positions between the vehicles more realistic and produces the scattered plots of the traffic output data. In addition, vehicles are also generated increasingly at the beginning of the simulation, 800 s, so as to achieve the maximum traffic rate. The traffic rate is then drawn from a normal distribution in which the mean decreases with the simulation time (see Eq. (5)). When the queue of waiting vehicles moves backward and approaches the original points, vehicle generation is temporarily stopped. This mechanism simulates the change in traffic from a free flow to a congested flow [18]. The simulation is set to run for 4 h.

$$Traffic\ rate\ (veh/s)$$
$$= \begin{cases} \dfrac{Time}{1600} & if\ Time \le 800\ s \\ Normal\left(\dfrac{800}{Time+800}, 0.25^2\right) & if\ Time > 800\ s \end{cases} \quad (5)$$

4.1.4. Model specifications

In this simulator, two different models are combined: a free acceleration model and the proposed motorcycle-following model. The rules for choosing which model to be used are as follows:

1) Free acceleration model
Each subject vehicle scans the area occupied by the pre-determined safety space so as to examine whether any influential vehicle exists inside the safety space. The boundary of the pre-determined safety space is assumed to be far enough for a subject motorcycle to perceive that it is unaffected by influential motorcycles, i.e., it feels free to accelerate its speed. Here, the boundary is supposed to be a

Table 3
Parameters for simulation.

Road size (length, width, in m)	(200.0, 5.4)
Traffic flow (veh/h)	From 0 to 5000
Free speed v_{max} (km/h)	28.8
A_{dec}	13.542
B_{dec}	0.132
A_{acc}	2.535
B_{acc}	5.269
Relaxation time τ (s)	0.498
Reaction time T (s)	0.5
Lateral distance W (m)	1.8
Vehicle size (meter length d_x, meter width d_y)	(1.9, 0.8)
Safety space for free acceleration (meter length L_{free}, meter width W_{free})	$(v_\alpha + 3.8, 2.6)$
Time required to change from the current speed to the maximum speed T_{free} (s)	1.5
Threshold distances in the emergency regime (meter length $L_{emergency}$, meter width $W_{emergency}$)	$(0.5v_\alpha + 1.9, 1.0)$
Lower bound of stopping distance before traffic signal L_{signal} (m)	20

rectangle with the length and the width denoted by L_free and W_free, respectively, as shown in Eq. (6).

$$\text{Pre−determined safety space} = \text{Length } L_{free}(m) \times \text{Width } W_{free}(m). \quad (6)$$

When no influential motorcycle or only one preceding motorcycle on the left or right is inside the pre-determined safety space, the subject motorcycle can run free or overtake freely the preceding motorcycle with the following acceleration rate:

$$a^x_{\alpha,free} = \frac{v_{max} - v^x_\alpha}{T_{free}}$$
$$a^y_{\alpha,free} = 0 \quad (7)$$

where $a^x_{\alpha,free}$, $a^y_{\alpha,free}$ are the free accelerations of a driver α along the x-axis and y-axis of the road, respectively, and v^x_α is the current speed along the x-axis. v_{max} is the free speed at which α wishes to run and its direction is parallel to the x-axis of the road. T_{free} is the time required to change from the current speed to the free speed.

2) Motorcycle-following model

If two or more influential vehicles are inside the pre-determined safety space, the acceleration rate of subject vehicle corresponding to the most influential vehicle is determined by Eqs. (4a) and (4b).

3) Emergency regime

This regime is used when a following vehicle applies the emergency brakes to avoid a collision with a preceding vehicle. In this study, we adopted the conventional regime proposed by Yang and Koutsopoulos [19]. If a preceding vehicle runs inside a space smaller than a pre-determined space with the $L_{emergency}$ and $W_{emergency}$ as the lengths of the semi-major and semi-minor axes, respectively, then a following vehicle will apply deceleration brakes to avoid collision.

4) Stopping regime before traffic signal

A traffic signal is installed at a point 180 m into the 200-m-long road segment. It is activated at the 801st second from the start of the simulation. The signal cycle of 60 s has three displays: red, yellow (2 s), and green. The length of the red light increases by 1 s after every 240 s of progress in the simulation. Hence, the simulation requires 4 h to capture all the changes of the red light that affect the traffic density. The output data on the traffic flow along a 100-m stretch of road behind the traffic signal are collected.

When a lead motorcycle detects a traffic signal from a stopping distance less than a pre-determined lower bound L_{signal}, it decides to keep running or slow down to stop just before the signal. While the signal is green or yellow, a driver proceeds past the signal if the moving time to the signal is shorter than the remaining yellow time. Otherwise, the driver starts applying the brakes to decelerate and stop before the stop line. When the traffic signal turns green, the lead vehicles accelerate freely from the stop line according to Eq. (7). The queuing vehicles follow the most influential leader according to Eq. (4a) and (4b).

4.2. Verification

In this section, we describe the verification of the simulator. The simulator reproduces non-lane-based movements including oblique following and swerving. Subsequently, the fundamental diagrams on non-lane-based movements from the simulation are verified.

A simulation was performed to test the original movements of motorcycles. Oblique following and swerving in a congested traffic situation were reproduced. The simulation conditions included a road segment 200-m-long and 5.4-m-wide. Traffic flow, which is drawn from a normal distribution as given by Eq. (5), varies from 0 to more than 5000 vehicles per hour. The free speed was set to 28.8 km/h. All motorcycles are assumed to be identical in size with homogeneous behaviors. The estimated parameters of the model for the case of Phan Dang Luu Street are shown in Table 3, along with other parameters used for the simulation.

Oblique following and swerving are confirmed from the trajectories.

4.2.1. Oblique following

A motorcyclist prefers to follow another vehicle at an oblique angle so as to achieve a larger safety space relative to the influential vehicle in front. This oblique following behavior of a motorcycle is shown in the time–space trajectories illustrated in Fig. 5. Each point in the figure represents the position of the most influential motorcycle or the subject motorcycle 0.5 s after the previous point. Many motorcycles are observed to maintain a small headway while following another along the road segment.

4.2.2. Swerving movement

This behavior shows a sudden swerving in response to changes in the speed of the lead vehicle. The simulated results showed that swerving is observed when motorcycles approach the signal. When the first motorcycles that detect the red light will decelerate to a stop, the following motorcycles slow down and swerve left or right to avoid colliding with the leaders. In the process, they reveal shock waves in the motorcycle traffic flow. The trajectory of a swerving motorcycle is illustrated in Fig. 6.

4.2.3. Fundamental diagrams

The simulation estimated the fundamental diagrams of motorcycle traffic flow at the road segment. The results are shown in Fig. 7. Because the free speed and reaction time are the same for all motorcycles, the dispersion of the output data is small. Motorcycles run at a free speed of around 28.8 km/h in the non-congested situation and then slow down to 1.0 km/h in response to congestion.

4.3. Effects of flow density on traffic conflict

In this section, simulations are performed to verify the effects of flow density on traffic conflict at a road segment.
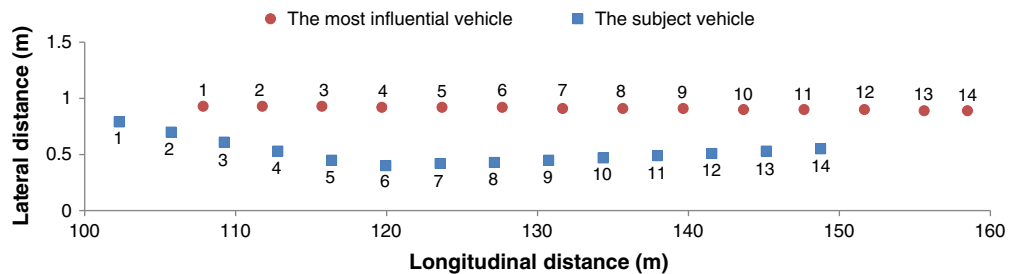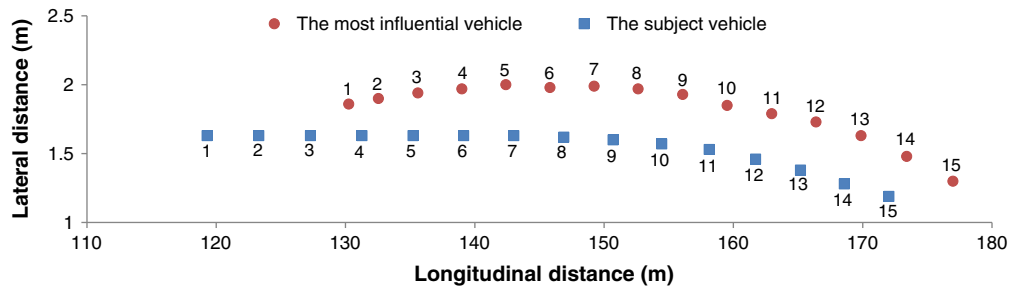

Fig. 5. Time–space trajectories of oblique following.

Fig. 6. Time–space trajectories of swerving movement.

4.3.1. Conflict situations at a road segment

Situations with many conflicts have a higher probability of accidents. In this study, we classified conflict situations under congested conditions into three basic types.
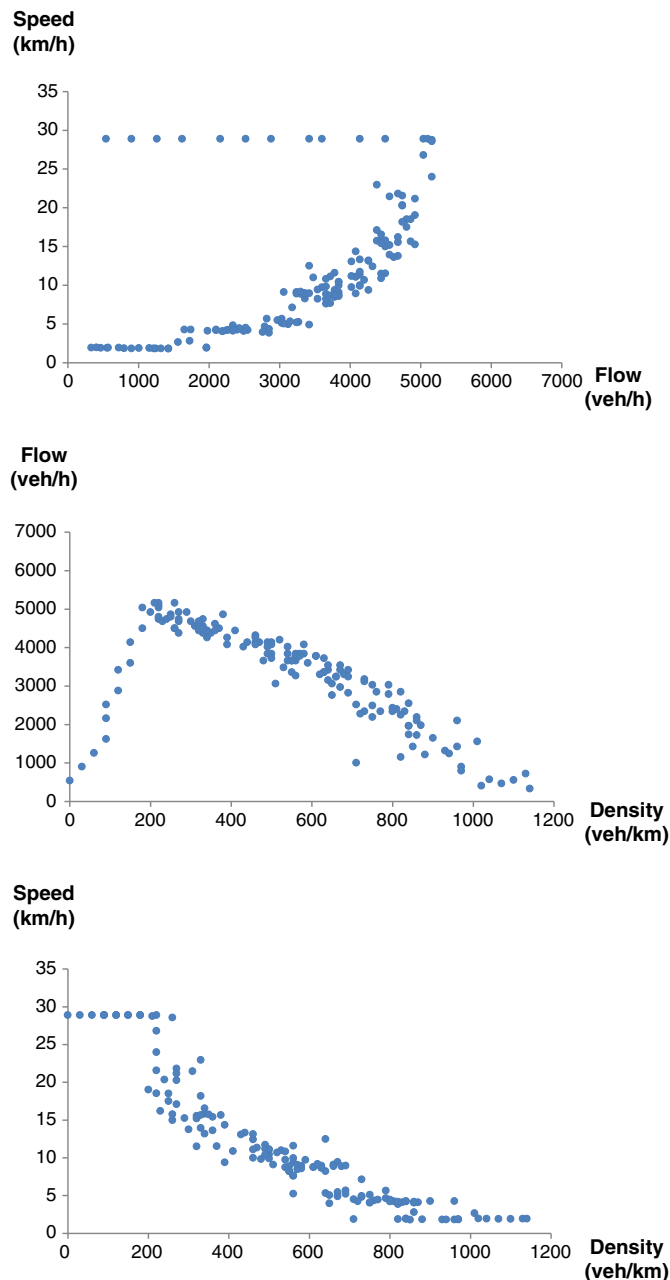

Fig. 7. Fundamental diagrams.

Type 1: A preceding vehicle suddenly changes speed and the following vehicle responds by applying the brakes and swerving away. If the relative speed between the two vehicles in the y-direction of the road is smaller than a given value of 0.25 m/s and the braking is inadequate to avoid a collision, the follower is assumed to crash into the rear of the preceding vehicle. The conflict could lead to a rear-end collision.

Type 2: A preceding vehicle suddenly applies the brakes and the following vehicle responds by applying the brakes and swerving away. If the relative speed in the y-direction of the road in is higher than a given value of 0.25 m/s and the braking is inadequate to avoid a collision, the side of one vehicle is assumed to be hit by the front or rear of another vehicle. The conflict could result in a T-bone side collision.

Type 3: Two side-by-side vehicles approach together from the left or right side. If the braking or swerving is inadequate to avoid a collision, the side of one vehicle is assumed to be hit by the side of another vehicle. The conflict could lead to a side-swipe collision.

On the basis of the classification above, each conflict type is assumed to correspond to a single collision type. However, correctly judging a type of collision by a conflict type is a challenge. In practice, when two vehicles collide, the true accident type will be confirmed by the position of the damaged parts on the body of the vehicles.

4.3.2. Conflict index: Deceleration rate

Several conflict indices are used to measure the frequency and severity of conflicts such as the gap time, TTC, and DR. Here, the DR is adopted as a conflict index for motorcycles. The DR is the value of the deceleration rate for a motorcycle when it applies the brakes to avoid a possible collision with other vehicles. If the DR exceeds a given critical value of 0.8 m/s^2, "sudden braking" is said to occur. This is an average deceleration value measured from the survey data. In this study, we calculate the probability of sudden braking for conflict assessment. This probability is defined as the percentage of observations in which a subject motorcycle applies a braking deceleration that exceeds the critical value across the total simulation time. Because the DR in an observation is measured for each 0.01 s time step, the probability of sudden braking can be calculated easily from the simulated results.

4.3.3. Effects of flow density on traffic conflict

The relationship between the probability of sudden braking and density is examined using survey data and simulation data. The survey data are based on observations from the video clips. Because a single observation at a certain time consists of only one subject motorcycle and its surrounding motorcycles, the Voronoi diagram is used to calculate the density at the position of the subject motorcycle. However, this method was not used for time saving in obtaining the density from simulation data. Instead, we used the average density in a 100-m-road segment at every time step of the simulation.

Voronoi diagrams permit density measurement on a very small spatial scale by assigning a space to a subject motorcycle. For each subject
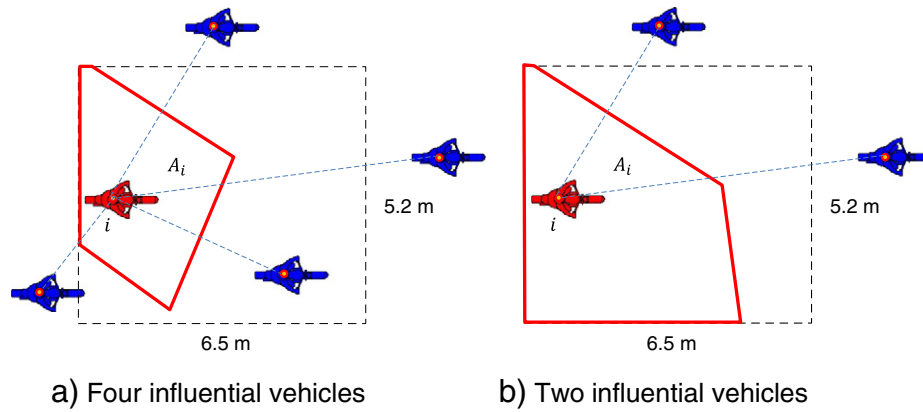
a) Four influential vehicles   b) Two influential vehicles

Fig. 8. Voronoi cell for motorcycle.

motorcycle, the flow density is calculated every 0.5 s. The space or Voronoi cell is defined as the area in which all the points are closer to the subject motorcycle than to the other motorcycles, as shown in Fig. 8. Voronoi diagrams have been used to determine the density of pedestrian traffic by Steffen and Seyfried [20]. The advantages of the method are that it: (1) estimates the instantaneous density at a given time point, and (2) addresses the problem of density scatter when the size of the motorcycle is comparable to that of the measuring area. Here, a Voronoi cell is assigned to each subject motorcycle through a Voronoi diagram. At a given time t corresponding to a certain observation, the density ρ_i (veh/m²) produced by a subject motorcycle i, positioned in relation to influential motorcycles, is determined by the Voronoi cell, A_i as follows:

$$\rho_i = \frac{1}{A_i}. \tag{8}$$

From the survey data, the influential motorcycles surrounding the subject motorcycle vary from 1 to 5 vehicles. A problem of applying Eq. (8) occurs when the number is relatively small (around 1 to 2 vehicles, as shown in Fig. 8b). Consequently, a Voronoi cell may extend to infinity. To deal with this problem, here we restrict the size of the Voronoi cell by a rectangle with a length of 6.5 m and a width of 5.2 m. These values are obtained from the average size of two semi-axes of the ellipsoid threshold safety space.

The relationship between the probability of sudden braking and density derived from survey data collected in two different road segments is shown in Fig. 9. The density of motorcycle flow ranges from 200 to 800 veh/km in both locations. Because the number of

observations is small, the probability of sudden braking was calculated as the density was increased by 50 veh/km. Fig. 9 reveals that a higher flow density led to a greater increase in the probability of sudden braking. This makes sense because when motorcyclists run close together, they perceive that safety spaces become smaller; hence, they press the brake pedals more often.

A simulation was performed with the parameters of Phan Dang Luu Street (Table 3). The relationship was adequately reproduced (Fig. 9). Many data points from the survey data of Phan Dang Luu Street were approximated by the simulation data. A similar result was obtained, i.e., the probability of sudden braking increased as the density increased. Moreover, the simulation could emulate a large range of changes in traffic density from a free flow (0 veh/km) to a highly congested flow (1200 veh/km). Under very congested conditions (from 1000 to 1200 veh/km), the probability of sudden braking does not increase. This is logical because in such high-density situations, motorcycles have less safety spaces to swerve left or right. Therefore, they simply run slowly to follow the leader.

Although the probability of sudden braking cannot be used to estimate the number of accidents, the increase in probability of sudden braking at high levels of flow density could reflect the increase in the probability of accident rates [9,21,22]. Further research to investigate the relationship between sudden braking and the number of traffic accidents should be considered.

4.3.4. Relationship between flow density and types of traffic conflicts

Three types of conflicts were confirmed via the simulations. Observations with sudden braking were counted from the simulated output
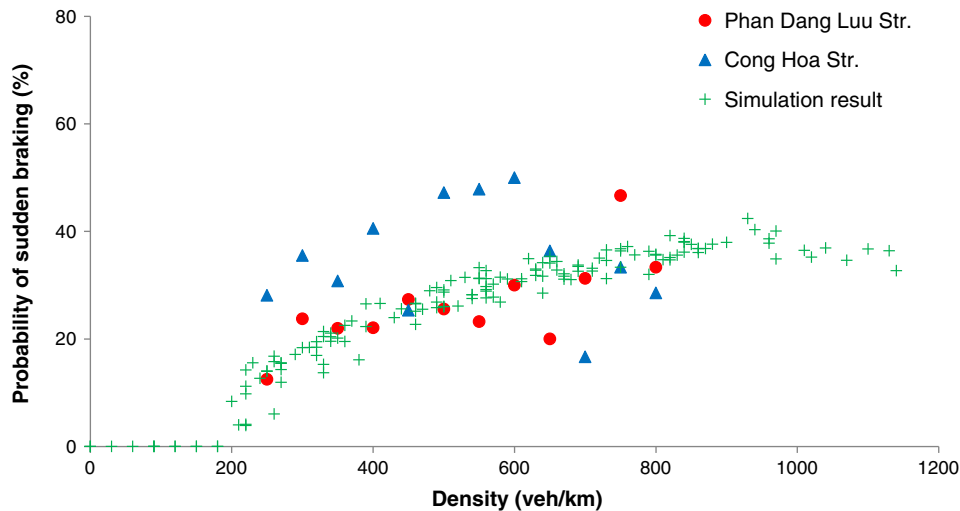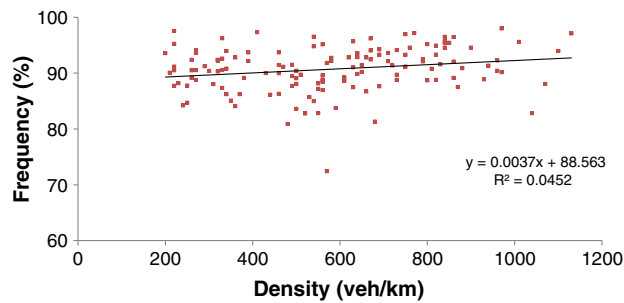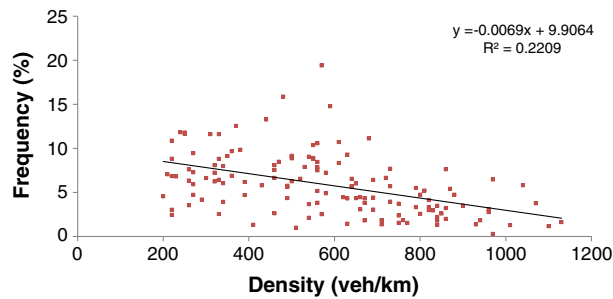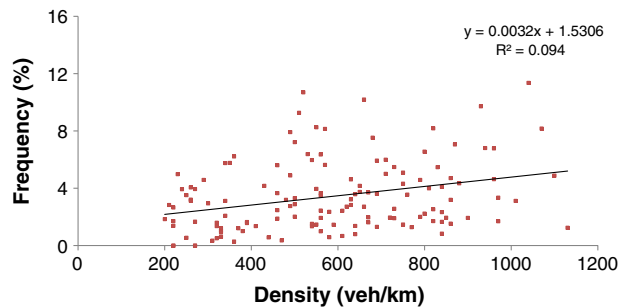

Fig. 9. Effects of flow density on probability of sudden braking.

y = 0.0037x + 88.563
R² = 0.0452

a) Type 1: Conflict leading to rear-end collision

y =-0.0069x + 9.9064
R² = 0.2209

b) Type 2: Conflict leading to T-bone side collision

y = 0.0032x + 1.5306
R² = 0.094

c) Type 3: Conflict leading to side-swipe collision

Fig. 10. Proportion of each type of conflict leading to collision in terms of flow density.

data and classified into three types of conflicts. The percentage of observations in each type of conflict among the total counted observations was calculated. Consequently, proportions of each conflict type were plotted against flow density (Fig. 10). Linear regression analysis was used to estimate the relationships between these variables. Nearly all parameters in the regression equations were significant at the level of 0.01, except for the first parameter of the regression equation for the type of conflict leading to rear-end collisions. Therefore, the average percentage of this type of conflict, which is stable at around 89%, is likely not related to the change in density. Conflicts leading to T-bone side collisions show a decreasing trend from 8% to 2% on average as the density increases. The proportion of conflicts leading to side-swipe collisions increases from 2% to 6% as the traffic flow becomes congested. Hence, the T-bone and side-swipe collisions appear to show a trade-off relationship. In high-density situations, a motorcycle has less space to swerve left or right; hence, the T-bone collision is unlikely to occur. In contrast, the proportion of motorcycles running side-by-side is greater; this leads to a higher likelihood of side-swipe collisions.

This result was discussed and compared to other statistical data. On the basis of data on motorcycle fatalities in Taiwan in 1997, Hsu et al. [23] proposed that side-swipe and rear-end collisions accounted for nearly 49% and 8%, respectively, of all fatalities. The report is likely to have collected data at both road segments and intersections. Turning left or right at intersections may be associated with a higher frequency of side-swipe accidents. However, conflicts at intersections are beyond the scope of this study. Padmanaban and Eyges [24] identified types of fatal motorcycle crashes by using FARS data collected in the U.S. during the years 1990–2007. They found that on average, frontal crashes, side impacts, rear impacts, and rollovers accounted for 79%, 17%, 3%, and 1%, respectively. The high proportion of frontal crashes likely involves collisions with cars or trucks. Further studies will be required to provide analyses of conflicts at intersections as well as conflicts of motorcycles with different types of vehicles.

5. Conclusions

In this study, we proposed a model to assess motorcycle traffic conflicts. The concept of safety space was used to describe the behaviors of increasing or decreasing speed. New features were developed for traffic conflict assessment. First, the difference in numerical values between acceleration and deceleration was represented by introducing two new parameter sets for acceleration and deceleration. Second, the conditions for selecting a leader to accelerate were described, such as the following angle and the following route width. The parameters of deceleration, acceleration, and relaxation time were estimated using trajectory data collected in two different road segments at Ho Chi Minh City. Almost all parameters are statistically significant at the 0.01 level and do not differ for different locations.

Conflict situations and a conflict index of the deceleration rate were introduced. A simulation model was developed to assess traffic conflict by calculating deceleration rates at each time step when the density of the motorcycle flow was changed. An assessment on traffic conflict is validated by calculating the probability of sudden braking in terms of the density of motorcycle flow. This finding underscores the fact that higher flow density led to a greater increase in the probability of sudden braking associated with a high risk of traffic accidents. Simulation results confirmed three types of conflicts. The proportion of conflicts leading to rear-end collision is likely to be constant, around 89%. Conflicts leading to a T-bone side collision show a decreasing trend, whereas those leading to a side-swipe collision increase slightly when traffic flow becomes congested.

The proposed model can be used to show non-lane-based or zigzag movements of motorcycles in cases where many influential vehicles are far enough for a subject motorcycle to distinguish the most influential vehicle clearly and respond to it on the basis of Assumption 3. Thus, a subject reacts to only one influential vehicle at a time. However, the subject vehicle may respond to two or more surrounding vehicles simultaneously, especially under very heavy traffic conditions. In reality, motorcycles show very smooth and clever movements when they run into small clearances, slightly wider than the width of a motorcycle, between two other preceding motorcycles. The model cannot replicate these movements. Instead, a subject motorcycle may express oscillatory movements in a short time as it slows down to react to the most influential vehicle on the left side, and then another on the right, in sequence. In the future, the proposed model will be improved to consider the extension of Assumption 3.

References

[1] D. Branston, Some factors affecting the capacity of a motorway, Traffic Eng. Control 18 (6) (1977) 304–307.
[2] S.A. Robertson, Motorcycling and Congestion: Definition of Behaviors, Contemporary Ergonomics, in: P.T. McCabe (Ed.), Taylor & Francis, London, 2002, pp. 273–277.
[3] H.J. Cho Cho, Y.T. Wu, Modeling and simulation of motorcycle traffic flow, IEEE International Conference on Systems, Man, and Cybernetics, 2004, pp. 6262–6267.
[4] C.C. Minh, K. Sano, S. Matsumoto, Deceleration models of motorcycles at signalized intersections, 85th Transportation Research Board Annual Meeting, Washington, D.C., 2006.
[5] C.C. Minh, K. Sano, S. Matsumoto, Maneuvers of motorcycles in queues at signalized intersections, J. Adv. Transp. 46 (1) (2010) 39–53.
[6] L.W. Lan, C.W. Chang, Inhomogeneous cellular automata modeling for mixed traffic with cars and motorcycles, J. Adv. Transp. 39 (3) (2005) 323–349.

[7] T.R. Neuman, J.C. Glennon, Cost-effectiveness of improvements to stopping-sight-distance safety problems, Transp. Res. Rec. J. Transp. Res. Board 923 (1983).

[8] L. Warshawsky-Livne, D. Shinar, Effects of uncertainty, transmission type, and driver age and gender on brake reaction and movement time, J. Saf. Res. 33 (2002) 117–128.

[9] D. Gettman, L. Head, Surrogate safety measures from traffic simulation models, 82th Transportation Research Board Annual Meeting, Washington, D.C., 2003.

[10] D. Perkins, J. Harris, Criteria for traffic conflict characteristics, Report GMF 632, General Motors Corp, Warren, MI, 1967.

[11] W. Glauz, D. Migletz, Application of traffic conflict analysis at intersections, NCHRP Report 219, Transportation Research Board, Washington D.C., 1980

[12] M. Parker, C. Zegeer, Traffic conflict technique for safety and operations, Engineers Guide, FHWAIP-026, FHWA, Washington, D.C., 1988

[13] FHWA, Traffic conflict techniques for safety and operations — course materials, NHI Course 38059, USDOT, Washington D.C., 1990

[14] L.X. Nguyen, S. Hanaoka, T. Kawasaki, Describing non-lane-based motorcycle movements in motorcycle-only traffic flow, Transp. Res. Rec. J. Transp. Res. Board 2281 (2012) 76–82.

[15] K.I. Alhmed, Modeling Drivers' Acceleration and Lane Changing Behavior, PhD thesis Massachusetts Institute of Technology, 1999.

[16] T. Toledo, H.N. Koutsopoulos, M. Ben-Akiva, Integrated driving behavior modeling, Transp. Res. C 15 (2007) 96–112.

[17] D. Helbing, P. Molnar, Social force model for pedestrian dynamics, Phys. Rev. E. 51 (5) (1995) 4282–4286.

[18] T.C. Lee, An Agent-based Model to Simulate Motorcycle Behavior in Mixed Traffic Flow, PhD thesis Imperial College, London, 2008.

[19] Q. Yang, N.H. Koutsopoulos, A microscopic traffic simulator for evaluation of dynamic traffic management systems, Transp. Res. C 3 (1996) 113–129.

[20] B. Steffen, A. Seyfried, Methods for measuring pedestrian density, flow, speed and direction with minimal scatter, Physica A 389 (2010) 1902–1910.

[21] FHWA, Relationships between traffic conflicts and accidents, Report FHWA/RD-84/042, Office of Safety and Traffic Operations Research and Development, Virginia, 1985.

[22] A. Kaub, Highway corridor safety levels of service based on annual risk of injury, 79th Transportation Research Board Annual Meeting, Washington, D.C., 2000.

[23] T.P. Hsu, N.X. Dao, F.M.S. Ahmad, A comparative study on motorcycle traffic development of Taiwan, Malaysia and Vietnam, J. East. Asia Soc. Transp. Stud. 5 (2003).

[24] J. Padmanaban, V. Eyges, Characteristics of motorcycle crash in the U.S. 4th IRTAS conference, Seoul, 2009.